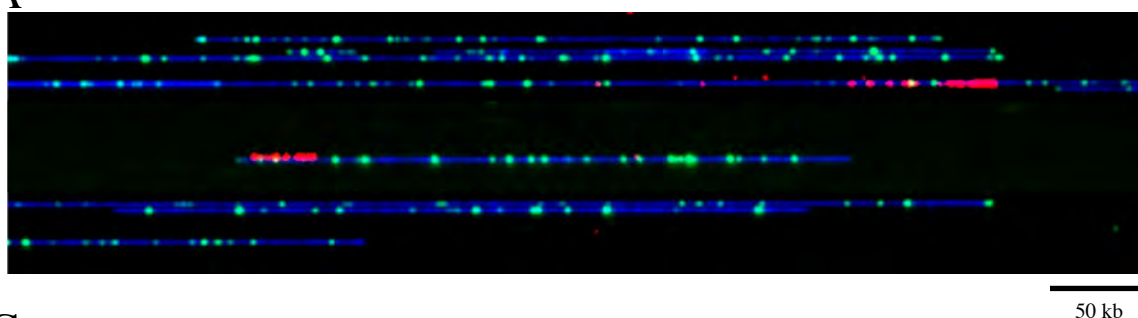
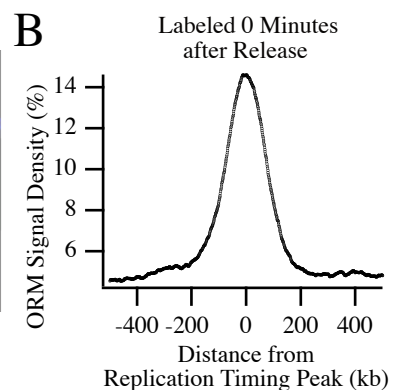


Figure 1

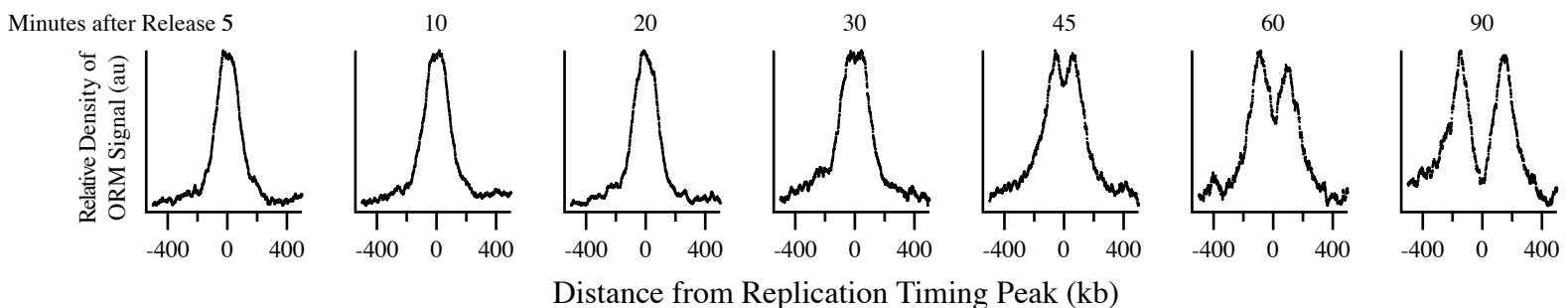
A



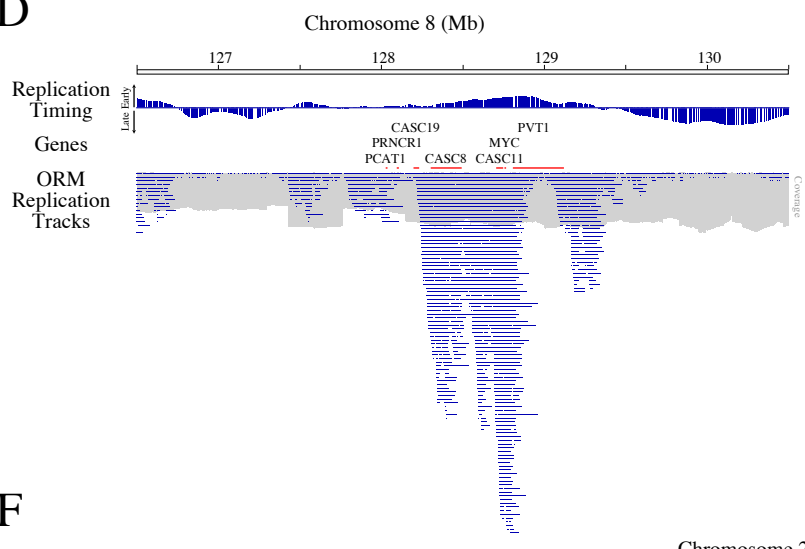
B



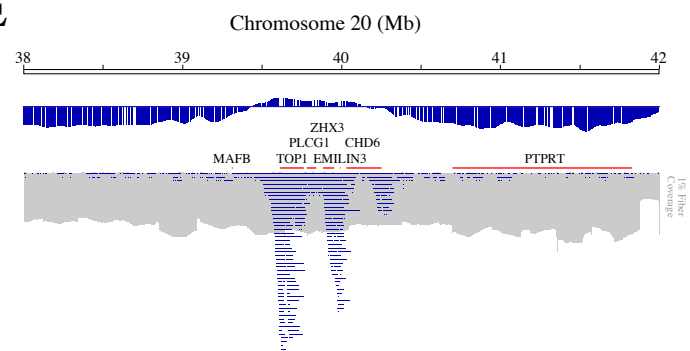
C



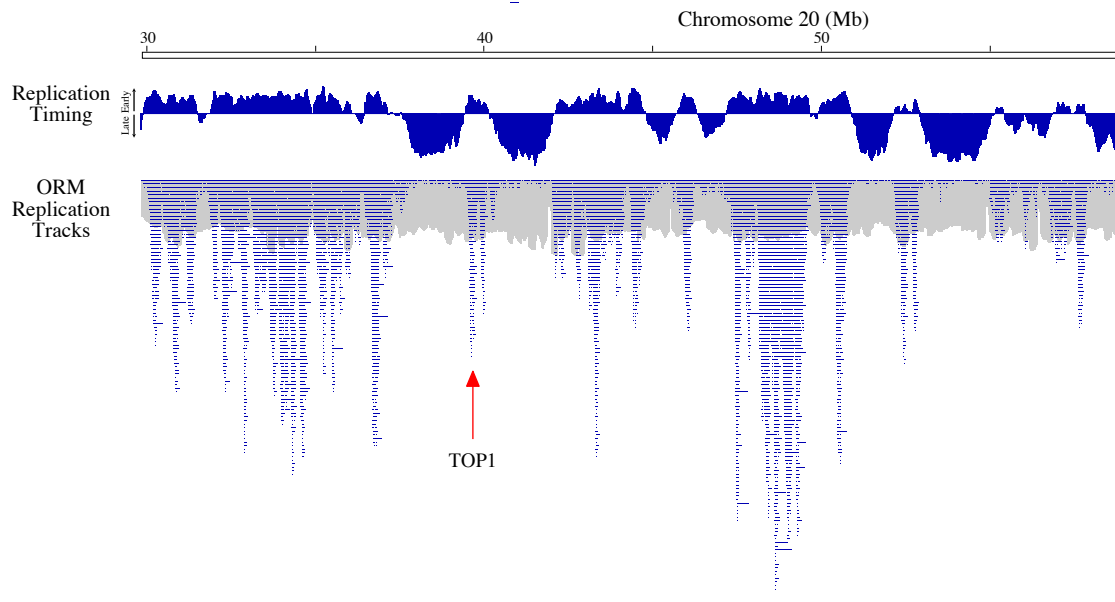
D



E



F



G

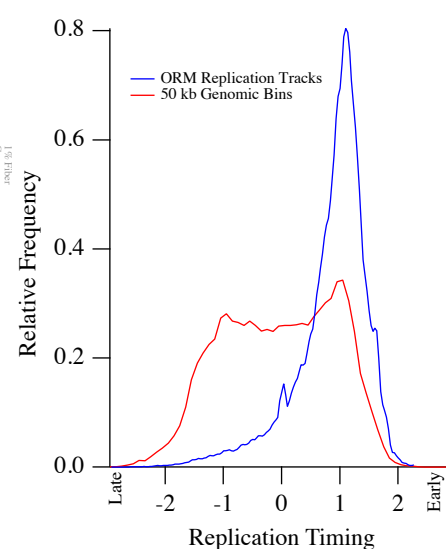
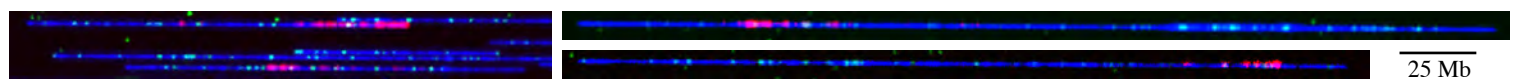
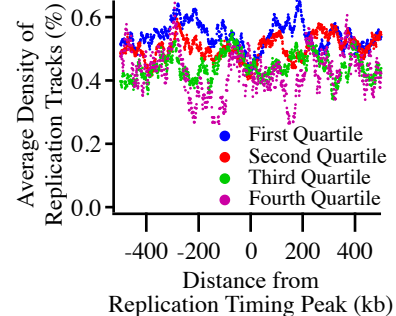


Figure 2

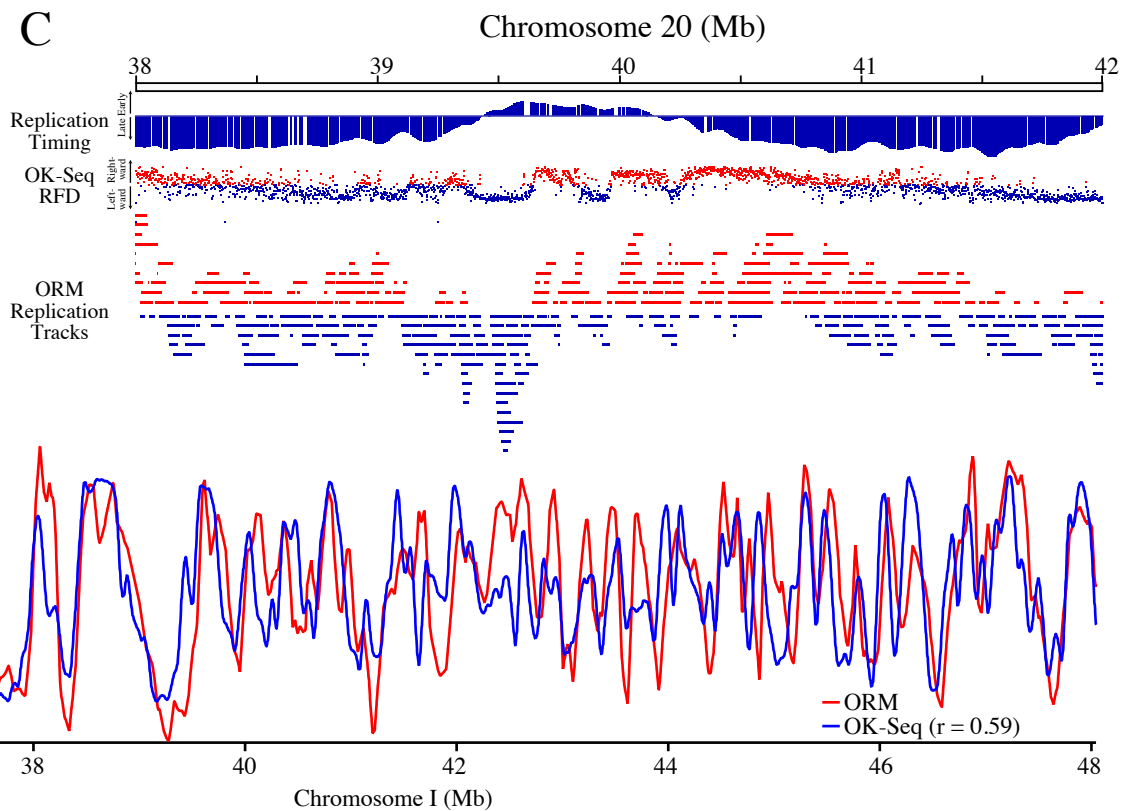
A



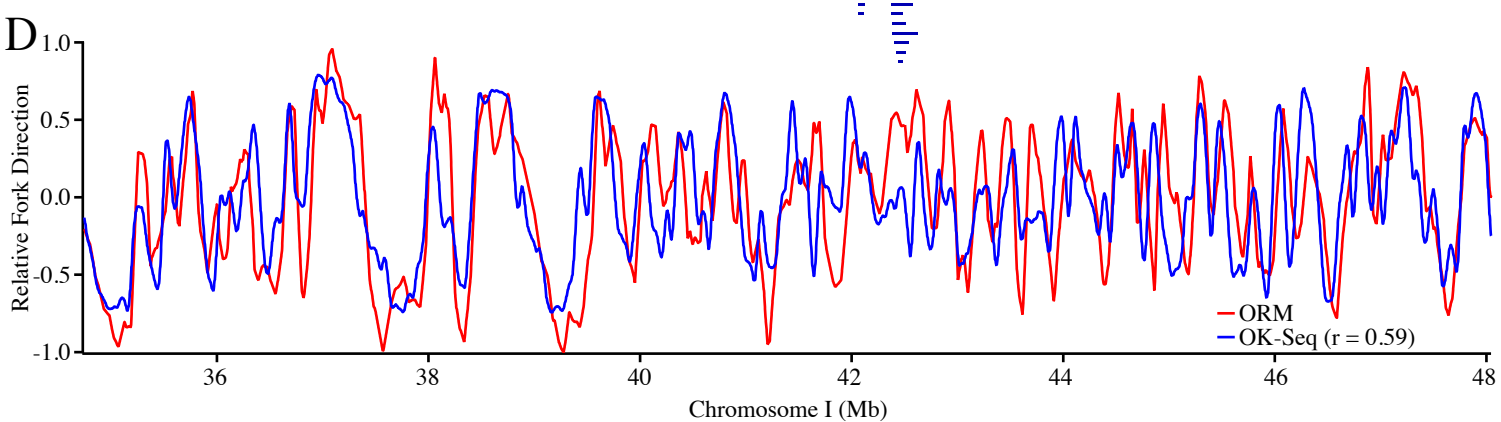
B



C



D



E

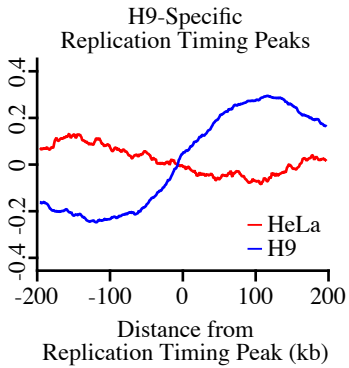
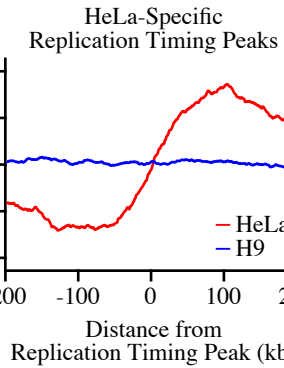
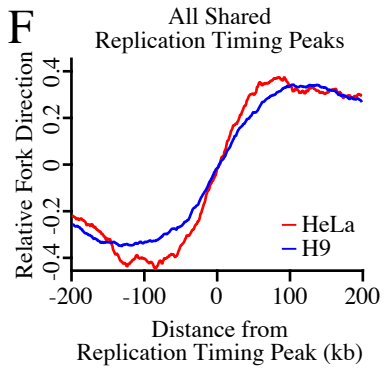
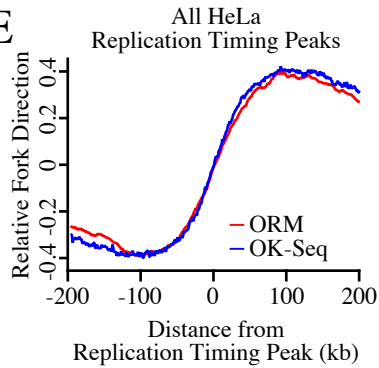
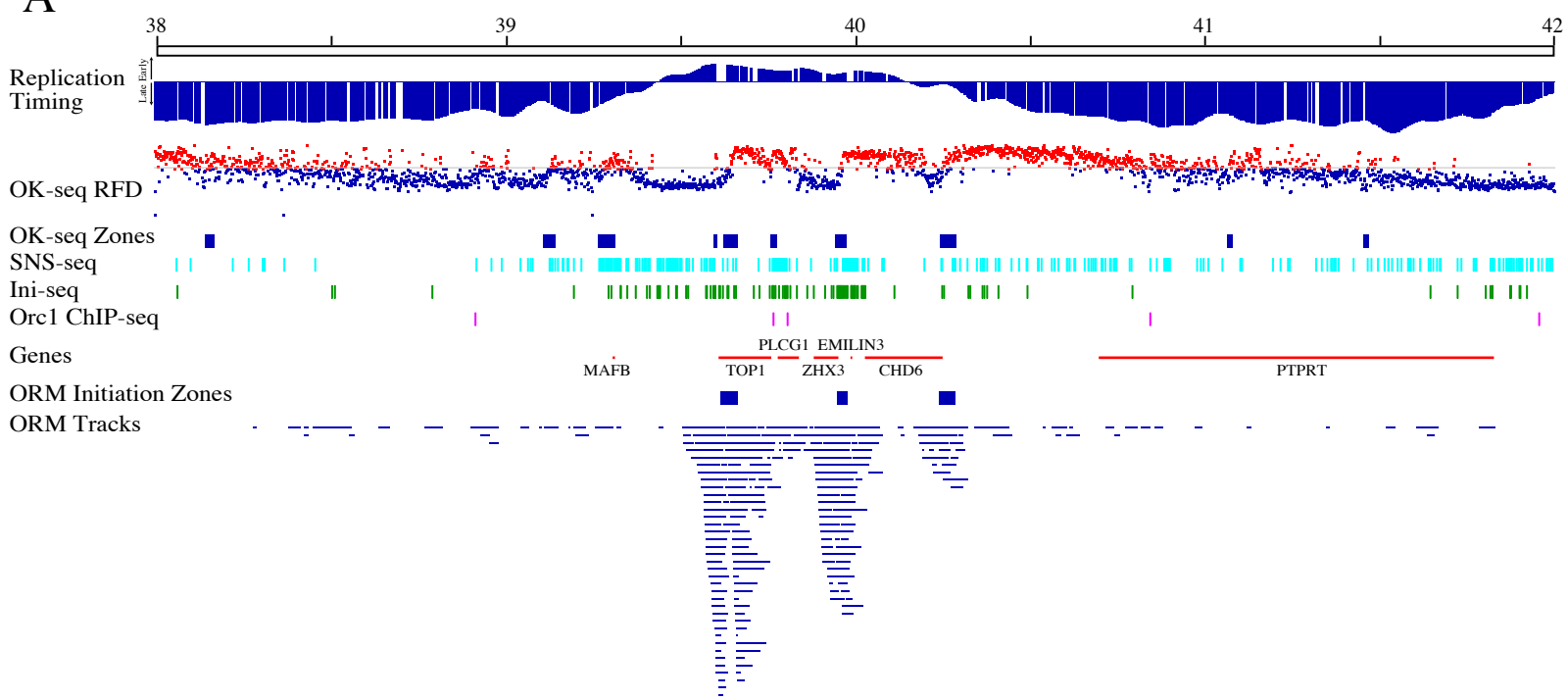


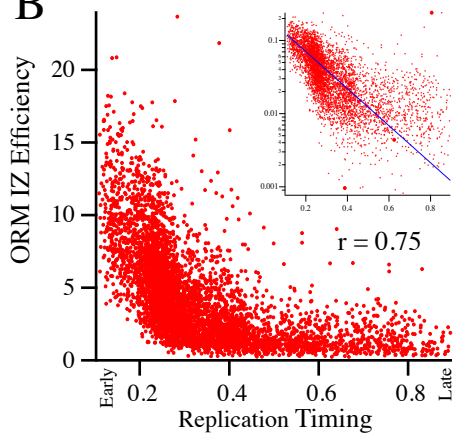
Figure 3

A

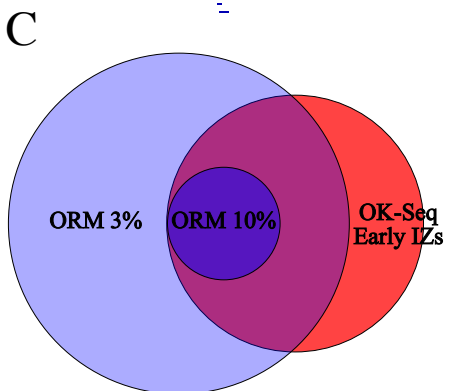
Chromosome 20 (Mb)



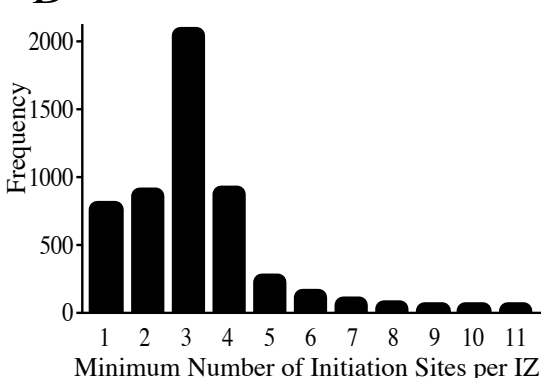
B



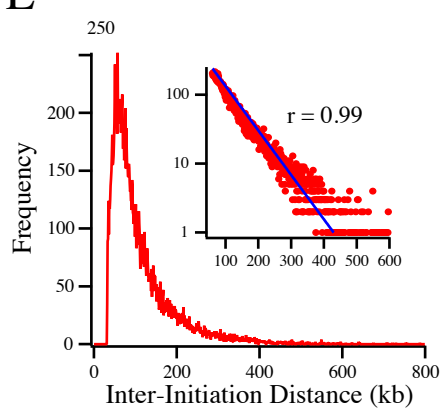
C



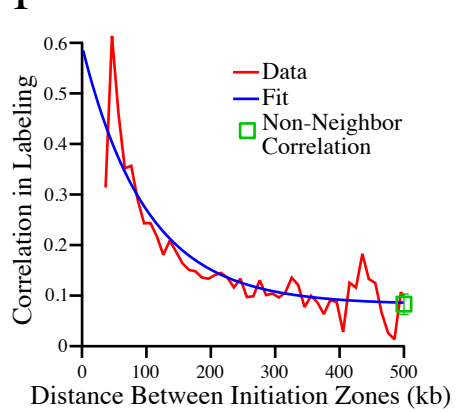
D



E



F



G

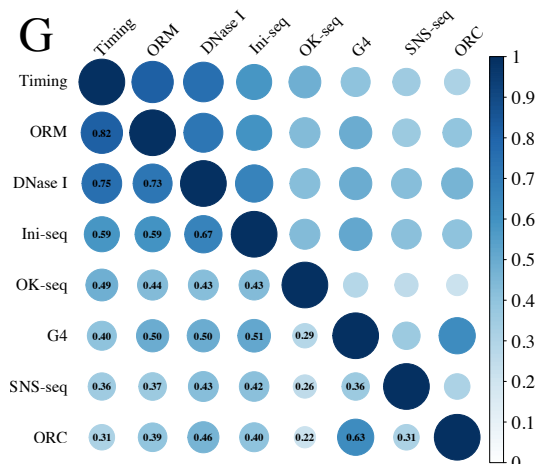


Figure 4

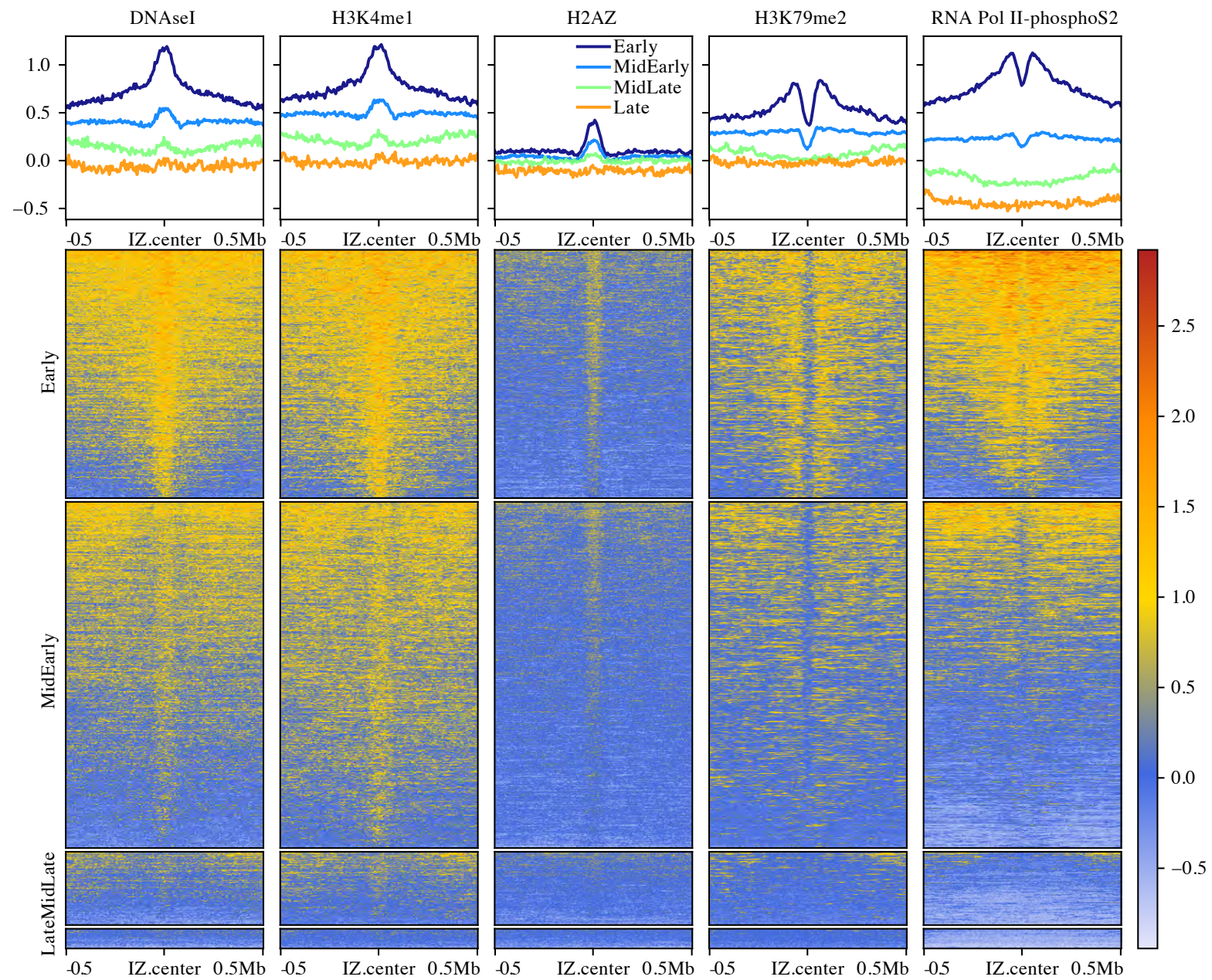


Figure 5

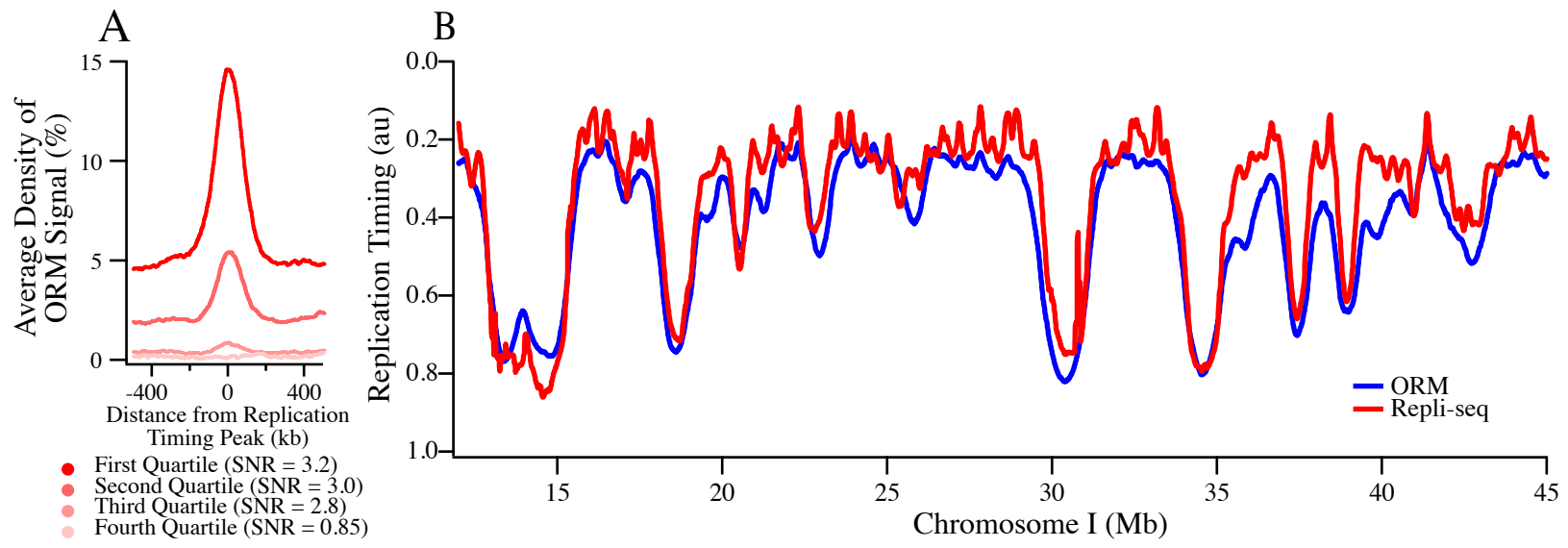


Figure S1

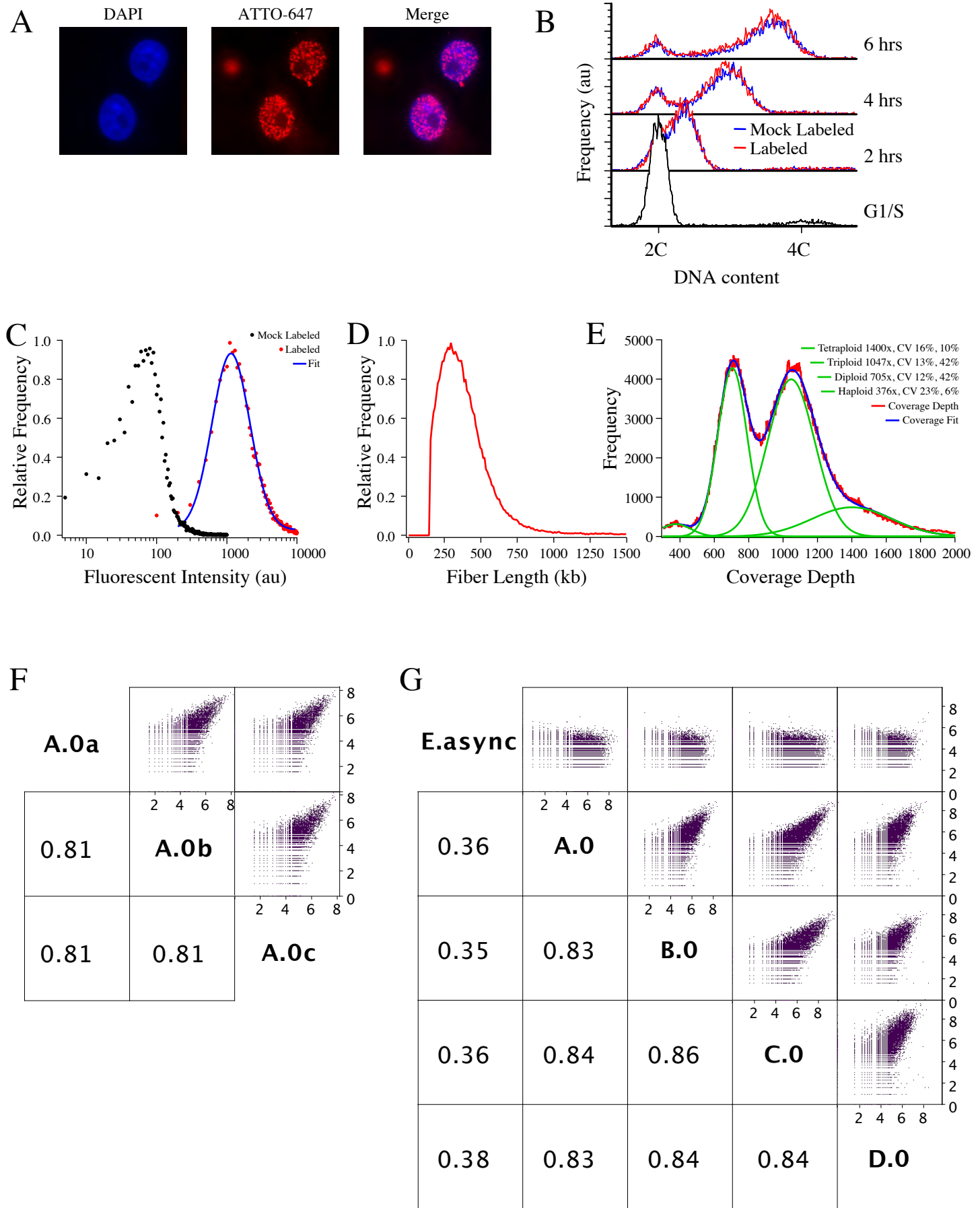
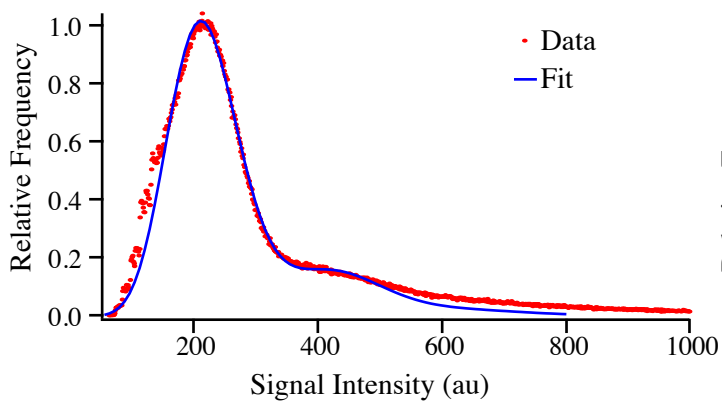
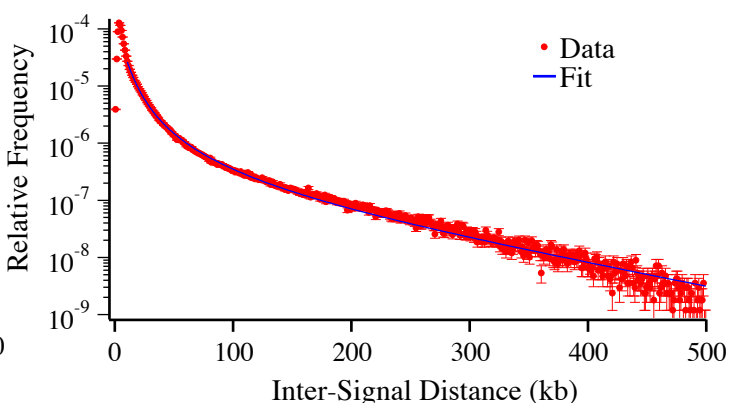


Figure S2

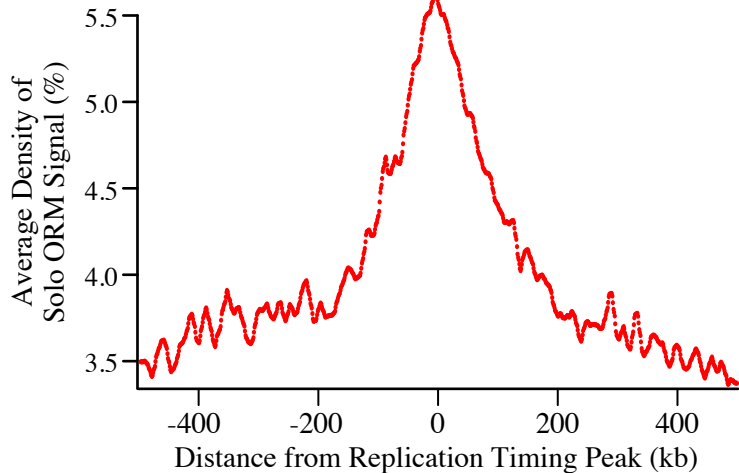
A



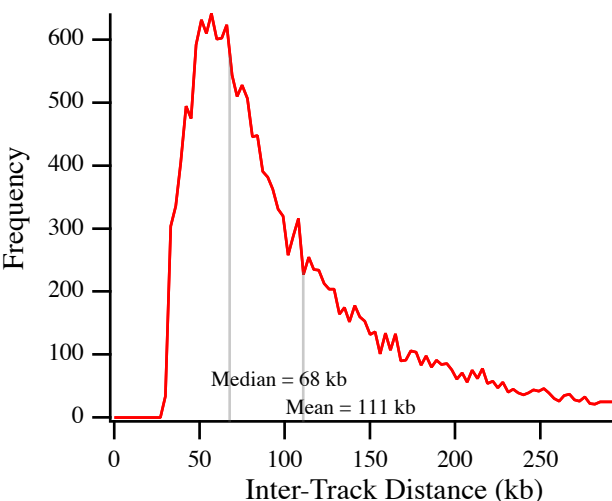
B



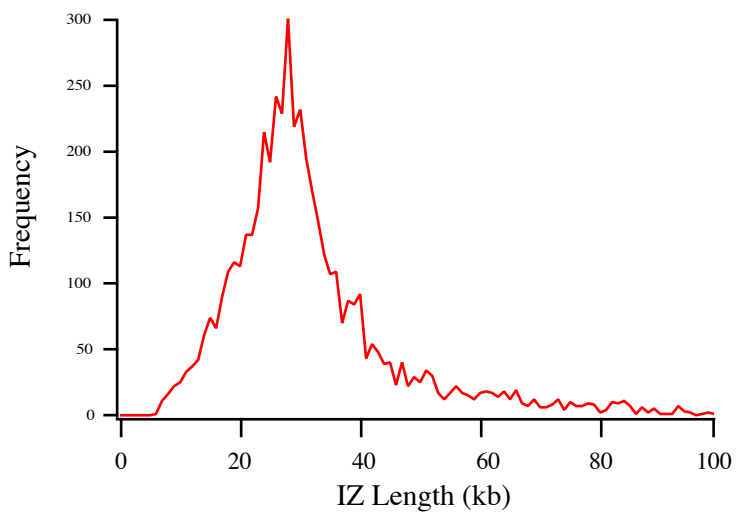
C



D



E



F

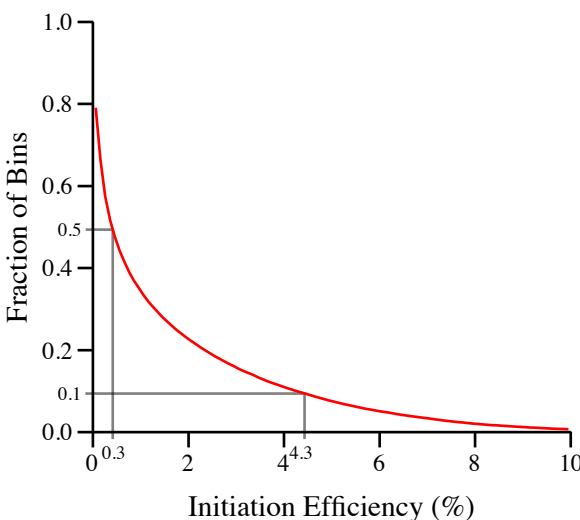


Figure S3

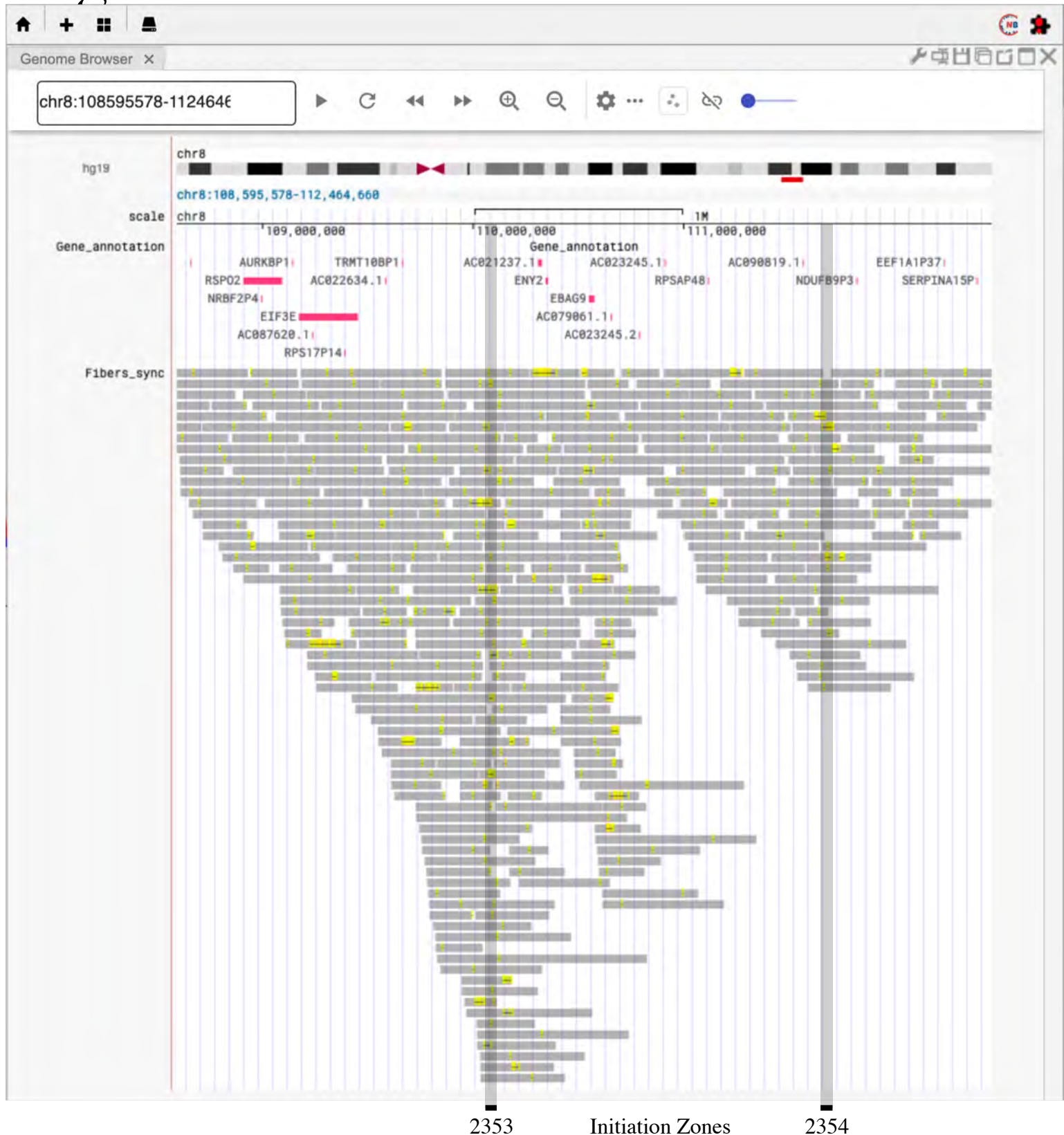
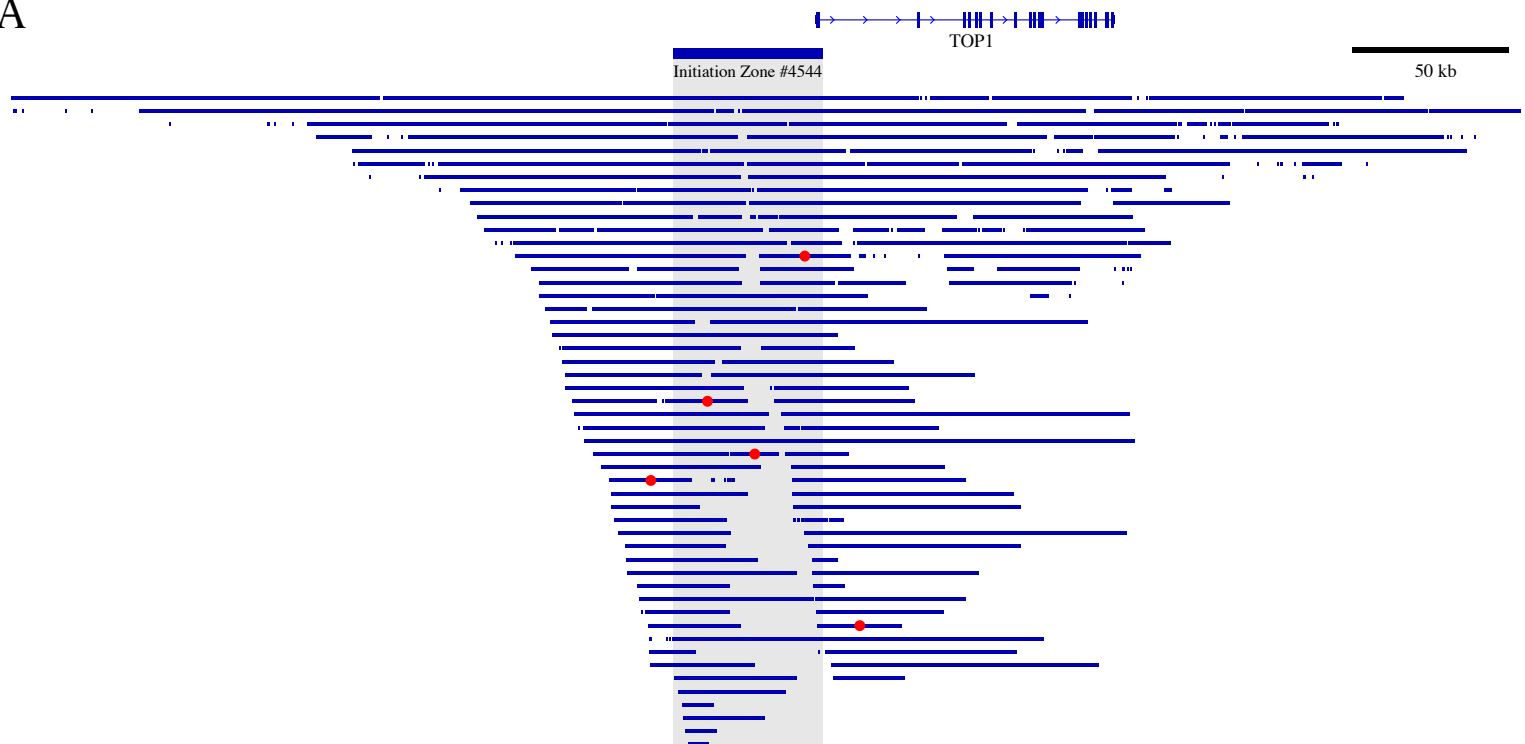


Figure S3. The ORM Genome Browser

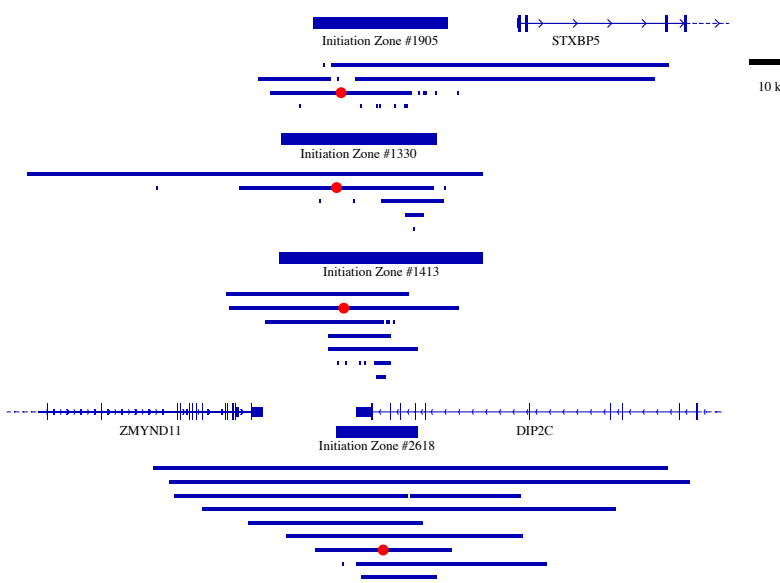
The ORM Genome Browser allows interactive visualization of the HeLa ORM data. Shown is a screen shot of the Fibers track of synchronous data. It shows fibers as gray bars, ORM signals as yellow hash marks, and inferred replication tracks as black lines. Only fibers labeled with ORM signals are displayed because only ~5% of fibers are labeled; displaying all fibers is impractical. The browser can also display only the replication tracks, to provide a more easily-visualized view of replication initiation. It can also show the fibers and the replication tracks from the asynchronous data. Two low-efficiency initiation zones are shown, 2353 (3%) and 2354 (2%), because higher-efficiency initiation zones contain too many labeled fibers. Note that, although the signals and replication tracks are concentrated around the initiation zones, many lay outside of them and none are concentrated in discrete areas.

Figure S4

A



B



C

Minimum Number of Initiation Sites per IZ

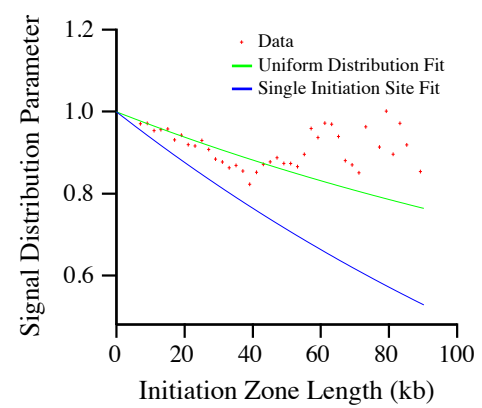


Figure S4. Distribution of Replication Tracks within Initiation Zones

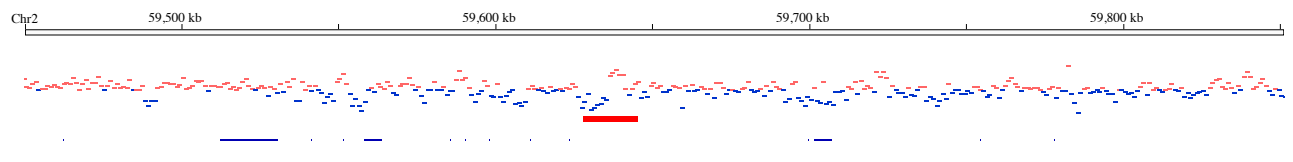
A) The distribution of replication tracks in the merged 0 minute dataset at the Top1 locus. The Top1 IZ has an estimated minimum of five initiation sites because the five replication track centers indicated in red are all 15 kb away from each other.

B) The distribution of replication tracks at four examples of IZs for which our estimate of the minimum number of initiation sites is 1.

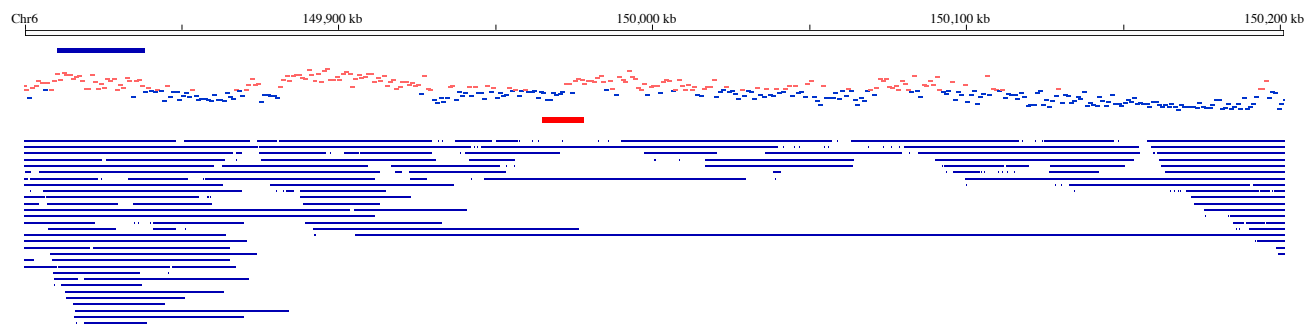
C) The distribution of signal across IZs. The ratio of signal frequency at the IZ center to the IZ boundary is plotted versus IZ length. This value is expected to decrease more quickly in IZs that predominantly have a single initiation site (Eq. 25) than if initiation is distributed across the IZ (Eq. 28, Supplemental Mathematical Methods). The distribution across IZs shorter than 55 kb is consistent with a uniform distribution of initiation sites. At longer lengths, we actually see more signal at the edges of the IZs than at the center. One possible explanation for this phenomenon is that larger IZs may actually be two smaller IZs fused together such that there is more initiation sites towards the edges of the fused IZ and less initiation in the center, which is actually between the two constituent IZs. See Supplemental Mathematical Methods for details.

Figure S5

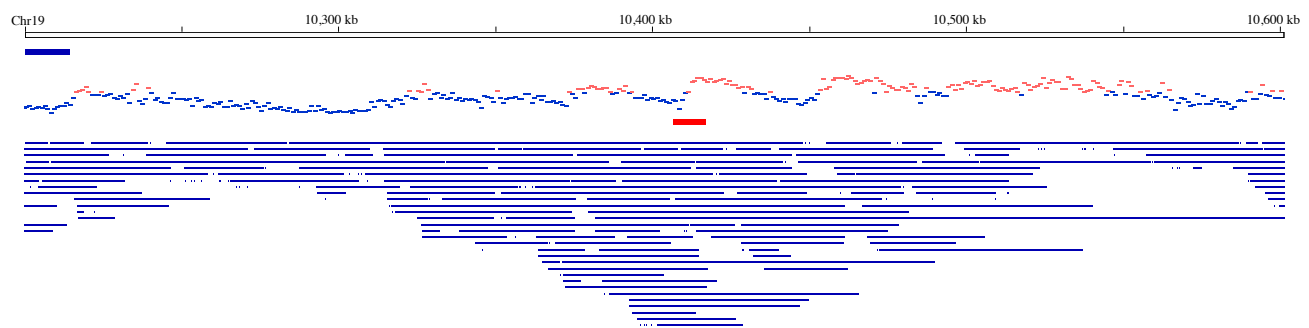
A



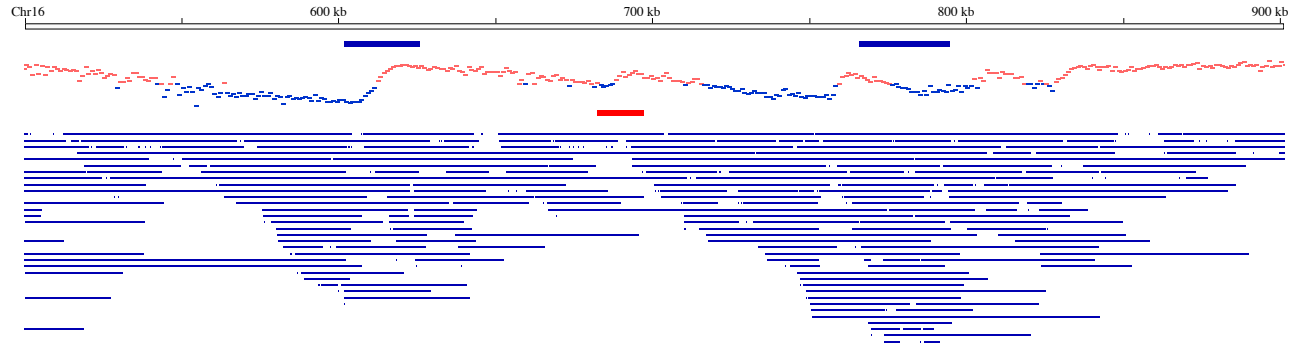
B



C



D



E

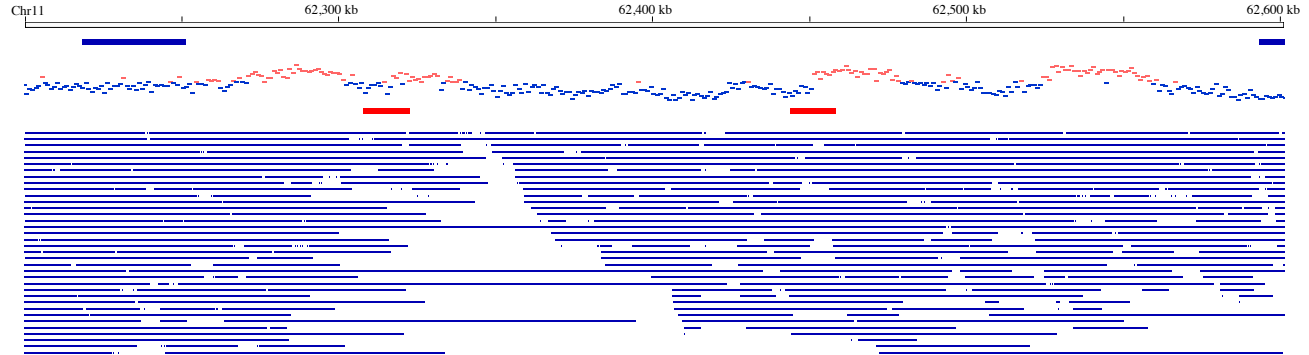


Figure S6

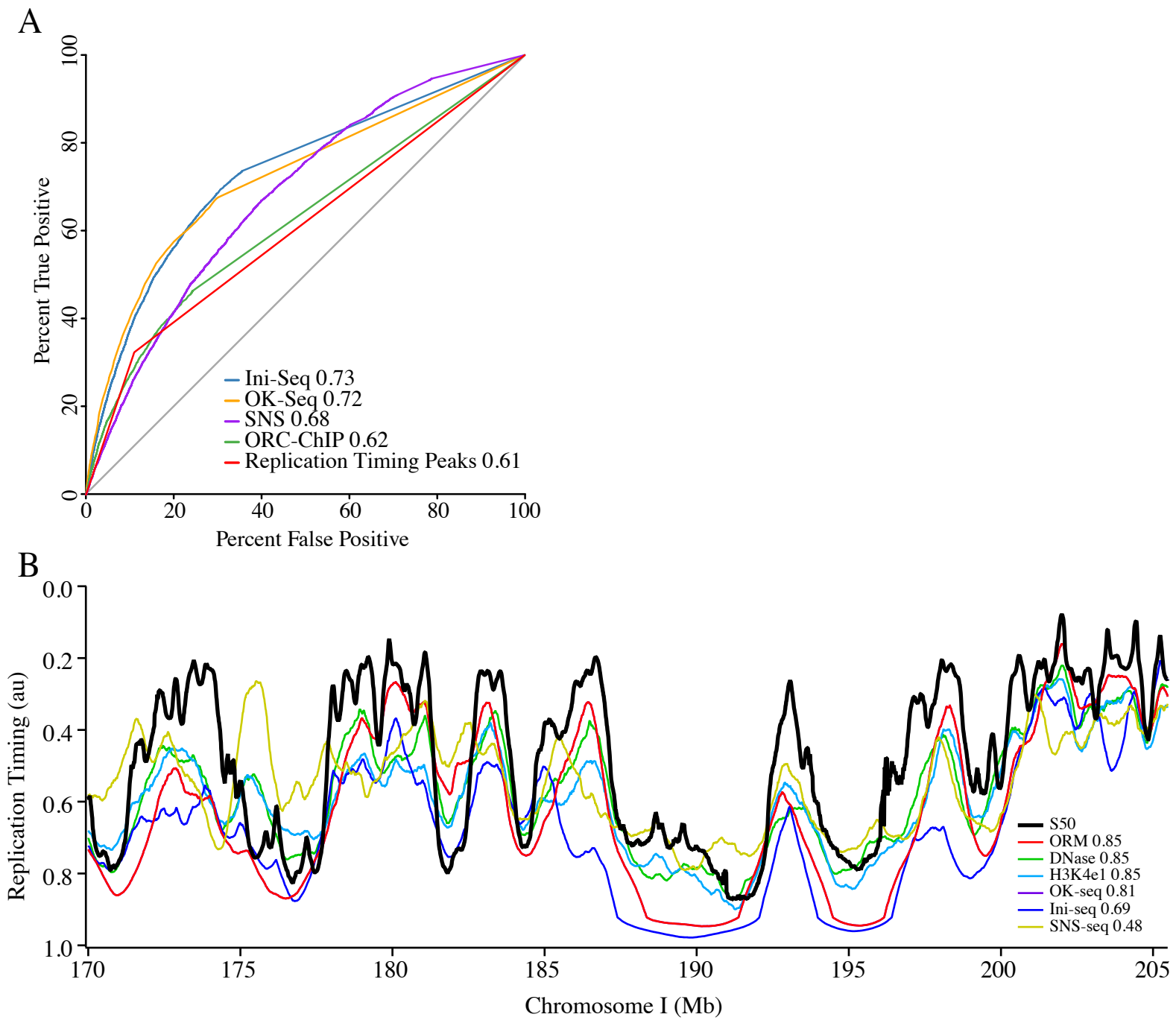


Figure S6. Simulated Replication Timing Profiles

A) ROC analysis of the association between the ORM IZs and other origin mapping data shown in Figure 3G. As shown in the ROC curves, the ORM IZs are better correlated with OK-seq IZs ($AUC=0.72$) and Ini-seq IZs ($AUC=0.73$). The bias of the SNS ROC curve towards high true positive rates only at high false negative values is consistent with that dataset having more false positive signal, whereas the bias of the replication timing and ORC datasets relatively high true positive rates only at low false negative values is consistent with those datasets having fewer, but more accurate true positives. Areas under the ROC curves (AUC) are shown in the legend.

B) Comparison between experimentally determined HeLa replication timing (S50) and replication timing predicted from ORM, DNase I hypersensitivity (Bernstein et al., 2012), OK-Seq (Petryk et al., 2016), Ini-seq (Langley et al., 2016) and SNS-seq (Picard et al., 2014) data using a stochastic model (Gindin et al., 2014a). The Spearman correlation coefficients with replication timing are shown in the legend.

Figure S7

